

# Feshbach Insulator from Atom-Molecule Coherence of Bosons in Optical Lattices

L. de Forges de Parny<sup>1</sup>, V.G. Rousseau<sup>2</sup>, and T. Roscilde<sup>1,3</sup>

<sup>1</sup> *Laboratoire de Physique, CNRS UMR 5672, École Normale Supérieure de Lyon, Université de Lyon, 46 Allée d'Italie, Lyon, F-69364, France*

<sup>2</sup> *Department of Physics and Astronomy, Louisiana State University, Baton Rouge, Louisiana 70803, USA, and*

<sup>3</sup> *Institut Universitaire de France, 103 boulevard Saint-Michel, 75005 Paris, France*

(Dated: December 7, 2024)

Feshbach resonances - namely resonances between an unbound two-body state (atomic state) and a bound (molecular) state, differing in magnetic moment - are a unique tool to tune the interaction properties of ultracold atoms. Here we show that the spin-changing interactions, coherently coupling the atomic and molecular state, can lead to a novel insulating phase - the *Feshbach insulator* - for bosons in an optical lattice close to a *narrow* Feshbach resonance. Making use of quantum Monte Carlo simulations and mean-field theory, we show that the Feshbach insulator appears around the resonance, preventing the system from collapsing when the effective atomic scattering length becomes negative. On the atomic side of the resonance, the transition from condensate to Feshbach insulator has a characteristic *first-order* nature, due to the simultaneous loss of coherence in the atomic and molecular components. These features appear clearly in the ground-state phase diagram of *e.g.* <sup>87</sup>Rb around the 414 G resonance, and they are therefore directly amenable to experimental observation.

PACS numbers: 05.30.Jp, 03.75.Hh, 67.85.Hj, 03.75.Mn

*Introduction.* Feshbach resonances offer an invaluable tuning knob to control quantum many-body phenomena in ultracold atoms [1]. An (unbound) state of two interacting atoms and a bound state - hereafter called molecule - are brought into resonance by the application of a magnetic field thanks to the different magnetic moments of the two states. As the two states are coupled by spin-changing interactions, their resonance allows to control the effective scattering length of unbound atoms both in magnitude and sign. This latter aspect has been widely used experimentally to explore quantum many-body phases [1–5] and to tune transitions between them [6, 7]. On the other hand the coherent coupling between atoms and molecules has been exploited *e.g.* to observe atom-molecule Rabi oscillations [8, 9]; at the theory level, this coupling is at the basis of the prediction of a quantum phase transition between mixed atom-molecule and purely molecular condensates [10–15].

A fundamental trait of the atom-molecule coupling is its non-linear nature: only *pairs* of atoms can be converted to molecules, leading to a strong density dependence of atom-molecule conversion. Here we shall show that, in the case of bosons in optical lattices, this aspect alone can drive the system towards a new insulating phase. Indeed the atom-molecule conversion can pin the particle density to two particles per site, opening a particle-hole gap in the spectrum and leading to insulating behavior. We dub this state of matter a *Feshbach insulator* (FI). It appears at a Feshbach resonance sufficiently narrow for the repulsive interaction to prevent the collapse of the atomic cloud. Atom-molecule conversion can be visualized as the coherent *pair* hopping of atoms into a fictitious, secondary lattice hosting the molecules (see Fig. 1). In this picture the

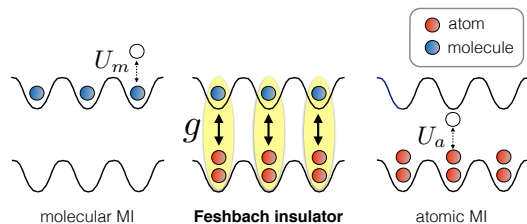


FIG. 1: (Color online) Various insulating phases appearing in the lattice atom-molecule coherent mixture. While atomic and molecular Mott insulators (MI) are stabilized by the repulsive interaction, the Feshbach insulator is stabilized by the atom-molecule coherence; yellow ellipses indicate superposition states between 2 atoms and a molecule.

mechanism stabilizing the FI is the appearance of strong entanglement between neighboring sites in the fictitious extra dimension, and the consequent suppression of entanglement in the real-space dimensions, which is instead at the basis of condensation. In dimensions  $D \geq 2$  the transition from a Bose-Einstein condensate of atoms and molecules (BECam) to the FI is found to have a strong first-order nature, as it is associated with the simultaneous restoration of two symmetries. We show that all these features are exhibited not only by an idealized model of atom-molecule resonance in optical lattices, but also by the phase diagram of <sup>87</sup>Rb close to its (narrow) 414 G resonance, and we discuss accessible experimental signatures of the FI and of the condensate-FI transition.

*Atom-Molecule Hamiltonian.* – We model spinless bosons in an optical lattice close to a narrow Feshbach resonance via a single-band Bose-Hubbard model (see note VI.1 of [16]) with atomic and molecular bosons,

coherently coupled via spin-changing atom-atom interactions [17]. The Hamiltonian of the system reads  $\hat{\mathcal{H}} = \hat{T} + \hat{P} + \hat{C}$ , where

$$\hat{T} = - \sum_{\langle i,j \rangle} \left( t_a a_i^\dagger a_j + t_m m_i^\dagger m_j + \text{H.c.} \right) \quad (1)$$

$$\hat{P} = \sum_i \left[ \frac{U_a}{2} n_i^a (n_i^a - 1) + \frac{U_m}{2} n_i^m (n_i^m - 1) + U_{am} n_i^a n_i^m + (U_a + \delta) n_i^m - \mu (n_i^a + 2n_i^m) \right] \quad (2)$$

$$\hat{C} = g \sum_i \left( m_i^\dagger a_i a_i + a_i^\dagger a_i^\dagger m_i \right). \quad (3)$$

The  $\hat{T}$  operator corresponds to the kinetic energy for hopping between nearest neighboring sites  $\langle i, j \rangle$  defined on a  $d$ -dimensional hypercubic lattice with periodic boundary conditions. The  $a_i^\dagger$  and  $a_i$  ( $m_i^\dagger$  and  $m_i$ ) operators are bosonic creation and annihilation operators of atoms (molecules) on site  $i$ . The  $n_i^a = a_i^\dagger a_i$  ( $n_i^m = m_i^\dagger m_i$ ) are the corresponding number operators. The  $\hat{P}$  operator contains the intra-species and inter-species interactions, as well as the chemical potential term; in particular it contains the detuning term  $\delta$ , which brings the state of two atoms and a molecule in and out of resonance on each site,  $\delta < 0$  corresponds to the molecular side of the resonance, while  $\delta > 0$  corresponds to the atomic side. Finally the  $\hat{C}$  operator is the hyperfine coupling converting two atoms into a molecule and viceversa.

The above atom-molecule Hamiltonian on a lattice has been mainly studied in  $D = 1$  [14, 15, 18, 19] for some peculiar choices of the numerous Hamiltonian parameters. Here we rather focus on the case of  $D = 2$  and 3 (see VI.2 of [16]), which we investigate numerically by a two-fold strategies: 1) in  $D = 2$ , we make use of numerically exact quantum Monte Carlo (QMC) simulations based on the Stochastic Green Function (SGF) algorithm with directed updates [20], both in a canonical and grand-canonical setting. We treat  $L \times L$  lattices with sizes up to  $L = 14$ . An inverse temperature of  $\beta t = 2L$  allows to eliminate thermal effects from the QMC results; 2) in  $D = 2$  and 3 we supplement the QMC calculations with Gutzwiller mean-field theory (MFT), consisting in solving the problem of a single site coupled to the self-consistent atomic and molecular mean fields,  $\phi_a = \langle a \rangle$  and  $\phi_m = \langle m \rangle$ , respectively. MFT is found to correctly capture the succession of phases in the system, and it allows for the rapid reconstruction of phase diagrams. The exact nature of the phase transitions encountered with MFT has been systematically investigated with QMC. The discussion of our results is structured as follows. We first focus on an idealized choice of Hamiltonian parameters, for which the FI is the *only* insulating phase appearing in the system. We then move on to investigating the occurrence of the FI phase for realistic parameters related to  $^{87}\text{Rb}$  in an optical lattice.

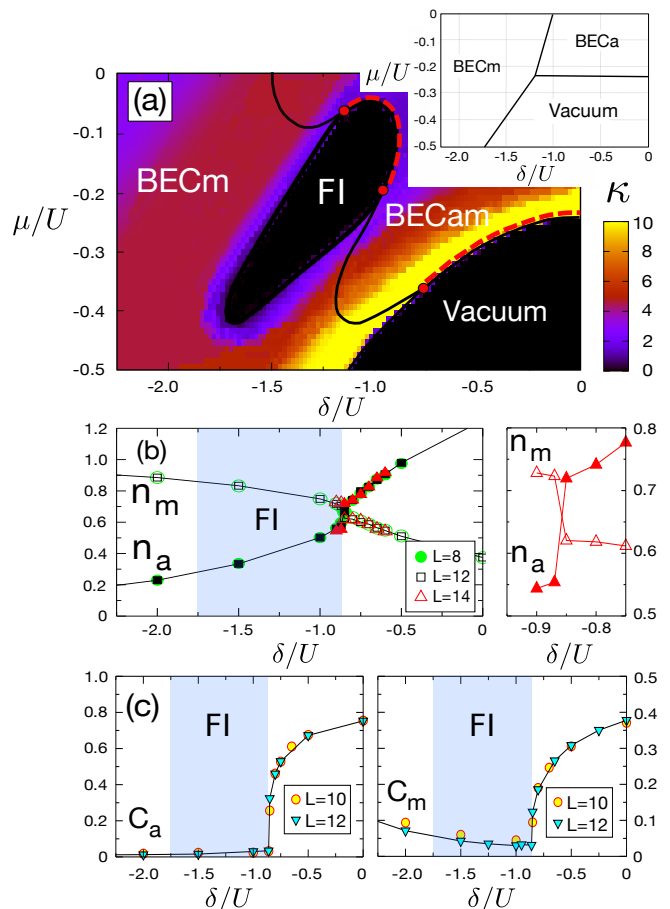


FIG. 2: (Color online) (a) Mean-field  $T = 0$  phase diagram of a symmetric atom-molecule mixture on a square lattice with  $t/U = 0.06$  and  $g/U = 0.8$  (false colors indicate the compressibility  $\kappa$ ). Inset: phase diagram for  $g = 0$ . Second-order transitions are denoted by solid black lines, red dashed lines indicated first-order transitions, and red dots denote tricritical points. (b) Atomic and molecular densities as a function of detuning. Results are from QMC simulations at fixed total density  $n = 2$ . Other parameters as in (a); (c) Atomic and molecular coherences as a function of detuning from QMC simulations. Parameters as in (b).

*Phase diagram of a 2D system.* – We begin our discussion of the ground-state physics by reducing enormously the choice of Hamiltonian parameters, imposing  $t \equiv t_a = t_m$  and  $U \equiv U_a = U_m = U_{am}$ . This establishes an (artificial) symmetry between the physics of atoms and molecules, which greatly simplifies the behavior of the system. Fig. 2(a) shows the phase diagram with fixed ratio  $t/U = 0.06$  as a function of the detuning  $\delta/U$  and of the total chemical potential  $\mu/U$ . If one neglects the coherent coupling  $g$  between atoms and molecules (inset of Fig. 2(a)) the only phases appearing in the system are an atomic BEC (BECa,  $\phi_a \neq 0$ ), a molecular BEC (BECm,  $\phi_m \neq 0$ ) and the vacuum – our specific choice of the  $t/U$  ratio does not allow for the appearance of finite-density

(Mott) insulating phases in this case. On the other hand, when  $g > 0$  ( $g/U = 0.8$  in Fig.2) the phase diagram changes dramatically [16]. The BECa phase turns into a phase hosting both an atomic and a molecular BEC (BEC<sub>m</sub>,  $\phi_a \neq 0$ ,  $\phi_m \neq 0$ ): at the mean field level this is easily understood in that the appearance of an atomic mean field  $\phi_a$  fixes the phase of the molecular field operators  $m$  through the conversion term  $C$ . The opposite is not true: a mean molecular field  $\phi_m$  fixes the phase of the *square* of the atomic field  $a^2$  only, fixing the phase of  $a$  only modulo  $\pi$  and leaving out an unbroken  $Z_2$  symmetry; whence the fact that a BEC<sub>m</sub> without atomic coherence (see VI.3 of [16]) persists in the phase diagram [10, 11, 13].

But the most striking feature of the phase diagram at  $g > 0$  is the occurrence of a broad FI region at fixed total density  $n = n_a + 2n_m = 2$  (see VI.4 of [16]). Its incompressible nature ( $\kappa = dn/d\mu = 0$ , see Fig. 2(a)) reveals the existence of a particle-hole gap, which is induced by the non-linear nature of the atom-molecule conversion (see VI.5 of [16]). An important ingredient for the stabilization of a *homogeneous* FI is the choice of a *narrow* Feshbach resonance. Indeed, given that the potential energy scales as  $\sim Un^2$  and the conversion energy scales as  $\sim gn^{3/2}$ , one finds that the two compensate each other at a density  $n^{1/2} \sim g/U$ . To achieve a homogeneous state, one needs therefore  $g/U \lesssim n^{1/2}$  ( $= \sqrt{2}$  for the example in question); if this is not the case, atoms tend to cluster on a few sites with a cluster density  $\sim (g/U)^2$ , and hence they gradually collapse as  $g/U$  grows [16].

The MFT results are quantitatively confirmed by our QMC simulations. In particular we focus on scans at fixed total density in the canonical ensemble - see Fig. 2(b,c) - and calculate the average atomic and molecular densities,  $n_a$  and  $n_m$  respectively, and the condensate densities of atoms and molecules,  $C_a = \frac{1}{L^4} \sum_{ij} \langle a_i^\dagger a_j \rangle$  and  $C_m = \frac{1}{L^4} \sum_{ij} \langle m_i^\dagger m_j \rangle$ . Both the QMC (Fig. 2(b)) and the MFT results show that, upon lowering  $\delta$ , the atomic and molecular densities show a clear *jump* at the onset of the FI, witnessing the first-order nature of the BEC<sub>m</sub>-FI transition. This also reflected in visible jumps of the condensate densities  $C_{a(m)}$ . The first-order nature of the transition is not specific to the transition to the FI, but it appears to be generic for all BEC<sub>m</sub>-to-insulator transitions [13]; these quantum phase transitions restore a composite  $U(1) \times Z_2$  symmetry - see VI.6 of [16].

As shown in Fig. 2(a), BEC<sub>m</sub>-BEC<sub>a</sub> is induced upon lowering the detuning  $\delta$ . This transition, captured also at the mean-field level, is related to the restoration of the  $Z_2$  symmetry associated with the phase of the atomic field, and it is therefore expected to belong to the  $d + 1$  Ising universality class. While the universality class cannot be correctly reproduced at the mean-field level, our QMC simulations show a very convincing scaling of the coherent fraction as  $C_a = L^{-2\beta/\nu} F_{C_a}(L^{1/\nu}|\delta - \delta_c|/U)$  with ex-

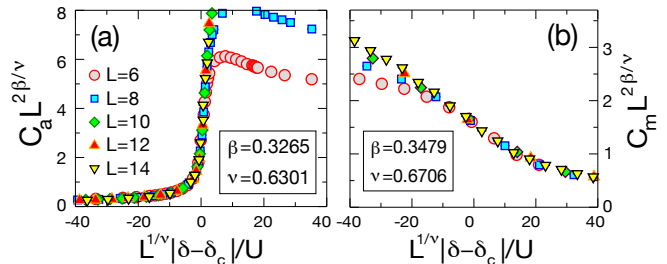


FIG. 3: (Color online) Scaling plots of the atomic and molecular coherences for the quantum phase transition from BEC<sub>m</sub> to BEC<sub>a</sub> at  $n = 0.5$  (a), and for the transition from BEC<sub>m</sub> to FI at  $n = 2$  (b), as obtained via QMC simulations. Other Hamiltonian parameters as in Fig. 2. Critical exponents of the 3D Ising (a) and 3D XY (b) universality classes [21], cited in the boxes, are used for the scaling.

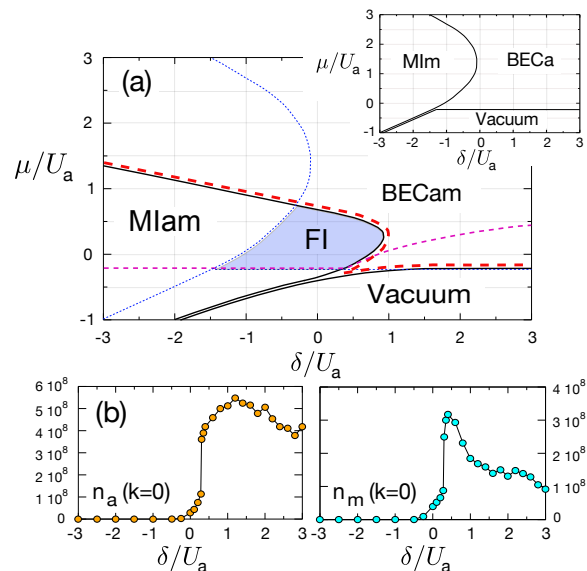


FIG. 4: (Color online) (a) Mean-field  $T = 0$  phase diagram for  $^{87}\text{Rb}$  close to the 414 G resonance in a cubic optical lattice of depth  $V_0 = 12E_r$ ; Inset: the same phase diagram obtained by artificially setting  $g$  to zero. (b) Peaks in the atomic and molecular distributions for a trapped system ( $\omega = 2\pi * 19 \text{ Hz}$ ) with central density  $\approx 1.96$  in the BEC<sub>m</sub> phase.

ponents  $\gamma$  and  $\nu$  belonging the 3D Ising universality class - see Fig. 3(a). When the detuning  $\delta$  is below the critical value for the onset of the BEC<sub>m</sub> phase, the insulator-condensate transition (FI-BEC<sub>m</sub> and vacuum-BEC<sub>m</sub>) loses the first-order nature characterizing the transition from the BEC<sub>m</sub> phase, and it becomes second order. Similarly to the single-species Bose-Hubbard model, it has mean-field exponents everywhere, except when it is realized at commensurate filling  $n = 2$  (lower tip of the FI domain) where the scaling of  $C_m$  is found consistent with the 3D XY universality class - see Fig. 3(b).

*Phase diagram of  $^{87}\text{Rb}$  in a lattice.* – We now turn our attention to a realistic implementation of the atom-molecule coherence model with a narrow Feshbach resonance, featuring most of the salient features observed in the previous, idealized example of a symmetric atom-molecule mixture. To make contact with most common experimental setups, we consider this time a 3D cubic optical lattice, and estimate the parameters  $t_a, t_m, U_a, U_m$  and  $U_{am}$  from atomic and molecular maximally localized Wannier functions [16]. The atom-molecule coherence  $g$  is estimated starting from the solution of the scattering problem for two particles in a harmonic potential [8, 16, 22]. We have focused on the two narrow resonances at 414 G in  $^{87}\text{Rb}$ , and at 853 G for  $^{23}\text{Na}$ , extensively investigated experimentally [8, 23, 24] - see VI.7 of [16]. The Hamiltonian parameters around these resonances have been estimated for a lattice depth  $V_0 = 12E_r$  (see VI.8 of [16]). We then scan the phase diagram as a function of chemical potential  $\mu$  (controlled by the trapping potential) and detuning  $\delta$  (controlled by the applied magnetic field), making use of mean-field theory (expected to be quantitatively accurate within some 10% in 3D systems). As the two resonances in  $^{87}\text{Rb}$  and  $^{23}\text{Na}$  feature a similar phase diagram, in the following we shall focus on the case of  $^{87}\text{Rb}$  only. For  $V_0 = 12E_r$  the microscopic parameters take values  $t_a/U_a = 0.04$ ,  $t_m/U_a = 3 \times 10^{-5}$ ,  $U_m/U_a = 12.9$ ,  $U_{am}/U_a = 3.24$  and  $g/U_a = 1.23$ . With this choice of the lattice depth, the atom-molecule conversion term is quite sizable ( $g \approx U_a$ ), yet a Mott insulator of atoms cannot be stabilized at any filling (neither at the mean-field level nor at the exact level [25]): therefore insulating behavior at finite density on the atomic side of the resonance is necessarily induced by the conversion term, namely it has the nature of a FI (see VI.9 of [16]).

Fig. 4(a) shows the mean-field phase diagram for  $^{87}\text{Rb}$  at the above cited resonance. In the absence of atom-molecule conversion (inset) the system features a BECa phase and a molecular MI (MIm) phase with  $n_m = 1$ . When  $g > 0$ , on the other hand, the BEC phase acquires a BECam nature, and similarly the MIm acquires an atomic component (MIam). The insulating region substantially shrinks on the molecular side, except for sufficiently low chemical potentials, where it is found to grow and appear even on the atomic side. This is a clear manifestation of the FI behavior. More specifically we identify with FI the region of the phase diagram which becomes insulating after  $g$  is turned on. Yet in the case at hand the FI is continuously connected with the more conventional MIm appearing for large negative values  $\delta$ . Suggestively, the FI appears exactly around the single-site resonance  $\delta = 0$ , and it spreads over a region of size  $\sim g$ , related to the width of the resonance.

The transition from the BECam to all the insulating phases is found to be strongly first-order. Remarkably, the unconventional nature of the BEC-insulator transition in this system can be directly observed in the ex-

periments using state-of-the-art diagnostics. Fig. 4(b) shows the evolution of the coherence peak across the BECam-FI transition for a trapped system with trapping frequency  $\omega = 2\pi * 19$  Hz,  $n_{a,m}(k=0) = \frac{1}{(2\pi)^3} \sum_{ij} \phi_{i,a(m)}^* \phi_{j,a(m)}$  (see VI.10 of [16]). The data for the local mean fields  $\phi_{i,a(m)}$  are obtained from single-site MFT via a local density approximation. The global chemical potential  $\mu_0$  is varied so as to maintain a fixed total density ( $n \approx 1.96$ ) in the trap center as  $\delta/U$  is varied (the density jumps to  $n = 2$  when entering in the FI phase); this leads to the trajectory shown as a thin dashed magenta line in Fig. 4(a). Along this realistic trajectory in parameter space we observe a very sharp jump of both the atomic and the molecular coherent peak as the trap center crosses the BEC-insulator transition (see VI.11 of [16]). A further accessible experimental evidence of the first-order nature of the BEC-insulator transition comes from the density profile. As shown in [16], when the trap center is in the FI phase, the density jumps twice upon moving towards the trap wings: once when going from FI to BECam, and a second time when going from BECam to vacuum.

*Conclusions.* We have shown that a narrow Feshbach resonance can introduce a novel insulating phase for bosons in an optical lattice – the Feshbach insulator – solely stabilized by the coherent atom-molecule coupling. The appearance of a thermodynamically stable Feshbach insulator shows that an optical lattice can actively protect the bosonic cloud against the two main enemies of ultracold resonant bosons in continuum space, namely 1) collapse on the attractive side of the resonance; 2) rapid three-body recombination on the repulsive side [26–28] – as triple occupancy of a site is largely suppressed in the FI. How to distinguish a Feshbach insulator from a conventional Mott insulator? As shown in the examples described above, FI behavior manifests itself for lattice depths at which atoms (and possibly even molecules) are far from a MI phase at all fillings: in this case, loss of atomic (and molecular) coherence upon tuning the system towards resonance is a clear manifestation of the appearance of a FI. Unlike conventional MI's, a FI consists of an almost equal mixture of atoms and molecules,  $\langle n_a \rangle \sim 2\langle n_m \rangle$  – an aspect directly accessible to experiments via Stern-Gerlach separation during the cloud expansion [29] or species-selective imaging [8]. Atom-molecule coherence can in principle be measured on small samples via the analysis of momentum-noise correlations between atoms and molecules [16].

*Acknowledgements.* We thank S. Dürr for useful discussions, and M. Eckholt-Perotti for her contributions at the early stages of this project. All calculations were performed on PSMN cluster (ENS Lyon). This work is supported by the ANR-JCJC programme (ArtiQ project).

## Supplementary Material: Feshbach Insulator from Atom-Molecule Coherence of Bosons in Optical Lattices

### ADDITIONAL INFORMATION ON THE MEAN-FIELD PHASE DIAGRAM

In this section, we provide additional elements concerning the mean-field phase diagram plot in Fig. 2(a) of the main text. The phase diagram is obtained by self-consistent minimisation of the following single-site Hamiltonian

$$\begin{aligned} \mathcal{H}_{\text{MF}} = & - (zt_a \phi_a a^\dagger + zt_m \phi_m m^\dagger + \text{H.c.}) \\ & + zt_a |\phi_a|^2 + zt_m |\phi_m|^2 \\ & + \frac{U_a}{2} n^a (n^a - 1) + \frac{U_m}{2} n^m (n^m - 1) \\ & + U_{am} n^a n^m + (U_a + \delta) n^m - \mu (n^a + 2n^m) \\ & + g (m^\dagger a a + a^\dagger a^\dagger m) \end{aligned} \quad (1)$$

where  $\phi_a = \langle a \rangle$  and  $\phi_m = \langle m \rangle$  are evaluated on the ground state of  $\mathcal{H}_{\text{MF}}$ ;  $z$  is the coordination number.

Fig. 1 shows the modulus of the atomic and molecular coherences ( $\phi_a$  and  $\phi_m$ ), exhibiting the presence of two distinct Bose-Einstein condensate (BEC) phase: atom-molecule BEC (BECam) and molecular BEC (BECm), separated by a continuous transition. Moreover two insulating phases are present: the vacuum phase and the Feshbach insulator (FI). Vertical cuts through this diagram, obtained by increasing  $\mu/U$  for two different values of  $\delta/U$ , are shown in Fig. 2. The cut at  $\delta/U = -1.4$  shows the continuous transitions between BECm and FI both for the atomic/molecular coherences as well as for the densities. On the other hand, the cut at  $\delta/U = -1$  shows that the BECam-FI transition (implying the breaking/restoration of a  $U(1) \times \mathbb{Z}_2$  symmetry) has a first-order nature, with clear jumps in both coherences and densities.

The first-order transition implies a coexistence between different phases. This can be clearly singled out at the mean-field level by setting  $\phi_a$  and  $\phi_m$  in the mean-field Hamiltonian Eq. (1) as parameters, and reconstructing the ground-state mean-field energy function  $E_{\text{MF}}(\phi_a, \phi_m)$  (both  $\phi_a$  and  $\phi_m$  are assumed to be real without loss of generality). Fig. 3 shows the mean-field ground-state energy  $E_{\text{MF}}$  as  $\mu/U$  is increased across the BECam-FI transition at  $\mu/U \simeq -0.23$  and  $\delta/U = -1.0$ . For  $\mu/U = -0.35$  (Fig. 3(a)) the energy landscape clearly shows three minima: two stables ones with  $\phi_a \neq 0$  and  $\phi_m \neq 0$  (corresponding to a BECam ground state), and a metastable one with  $\phi_a = 0$  and  $\phi_m \neq 0$  (corresponding to a metastable BECm). The three minima exhibit the strong asymmetry present between atoms and molecules due to the atom-molecule conversion term: when the phase of the molecular field is fixed (to zero in this

- 
- [1] C. Chin *et al.*, Rev. Mod. Phys. **82**, 1225 (2010).
  - [2] M. Greiner, *et al.*, Nature **426**, 537 (2003).
  - [3] M. Randeria and E. Taylor, Ann. Rev. Cond. Matt. **5**, 209 (2014).
  - [4] W. Ketterle and M. W. Zwierlein, in *Ultracold Fermi Gases, Proceedings of the International School of Physics "Enrico Fermi", Course CLXIV*, M. Inguscio, W. Ketterle, and C. Salomon (eds.), IOS Press, Amsterdam, 2008.
  - [5] K. Winkler *et al.*, Nature **441**, 853 (2006).
  - [6] R. Jördens *et al.*, Nature **455**, 204 (2008).
  - [7] B. Deissler *et al.*, Nature Phys. **6**, 354 (2010).
  - [8] N. Syassen *et al.*, Phys. Rev. Lett. **99**, 033201 (2007).
  - [9] M. L. Olsen *et al.*, Phys. Rev. A **80**, 030701(R) (2009).
  - [10] L. Radzihovsky *et al.*, Phys. Rev. Lett. **92**, 160402 (2004).
  - [11] M. W. J. Romans *et al.*, Phys. Rev. Lett. **93**, 020405 (2004).
  - [12] K. Sengupta and N. Dupuis, Europhys. Lett. **70**, 586 (2005).
  - [13] L. Radzihovsky *et al.*, Ann. Phys. **323**, 2376 (2008).
  - [14] S. Ejima *et al.*, Phys. Rev. Lett. **106**, 015303 (2011).
  - [15] M. J. Bhaseen *et al.*, Phys. Rev. A **85**, 033636 (2012).
  - [16] See Supplementary Material for: 1) further characterization of the mean-field phase diagram; 2) a discussion of the gradual passage from Feshbach insulator(s) to collapse; 3) a discussion of the Hamiltonian parameters extracted from the Wannier functions of a cubic optical lattice; 4) density profiles of  $^{87}\text{Rb}$  in a trap; 5) extraction of atom-molecule coherence from momentum-noise correlations; 6) further Information.
  - [17] T. Köhler, K. Góral, and P. S. Julienne, Rev. Mod. Phys. **78**, 1311 (2006).
  - [18] V. G. Rousseau and P. J. H. Denteneer, Phys. Rev. A **77**, 013609 (2008); V. G. Rousseau and P. J. H. Denteneer, Phys. Rev. Lett. **102**, 015301 (2009).
  - [19] M. Eckholt and T. Roscilde, Phys. Rev. Lett. **105**, 199603 (2010).
  - [20] V. G. Rousseau, Phys. Rev. E **77**, 056705 (2008); V. G. Rousseau, Phys. Rev. E **78**, 056707 (2008).
  - [21] A. Pelissetto and E. Vicari, Phys. Rep. **368**, 549 (2002).
  - [22] Th. Busch *et al.*, Found. Phys. **28**, 549 (1998).
  - [23] S. Inouye *et al.*, Nature **392**, 151 (1998).
  - [24] J. Stenger *et al.*, Phys. Rev. Lett. **82**, 2422 (1999).
  - [25] B. Capogrosso-Sansone *et al.*, Phys. Rev. B **75**, 134302, (2007).
  - [26] B. S. Rem *et al.*, Phys. Rev. Lett. **110**, 163202 (2013).
  - [27] R. J. Fletcher *et al.*, Phys. Rev. Lett. **111**, 125303 (2013).
  - [28] P. Makotyn *et al.*, Nature Phys. **10**, 116 (2014).
  - [29] J. Herbig *et al.*, Science **301**, 1510 (2003).

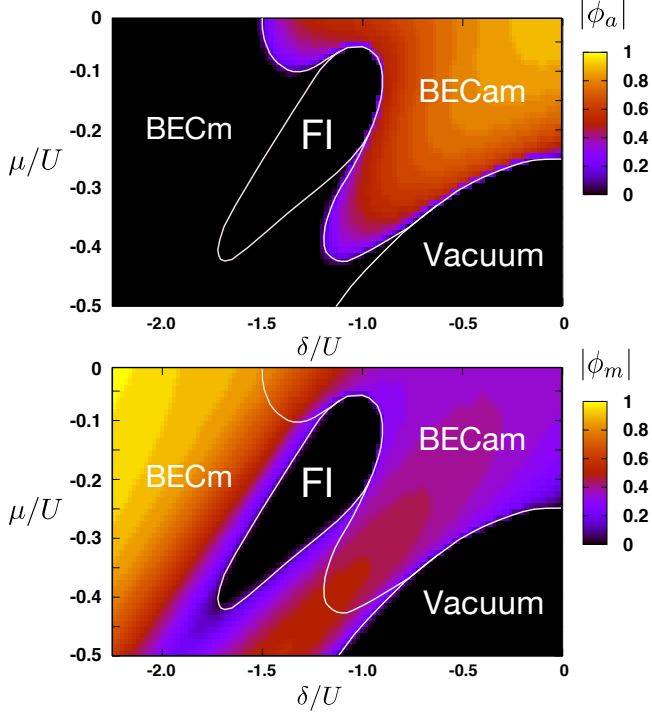


FIG. 1: (Color online) Modulus of the atomic (up) and molecular (down) coherences from the mean-field phase diagram plot in Fig.2(a) of the main text. The atomic coherence vanishes continuously at the BECam to BECam transition (upper panel) whereas the molecular coherence remains finite (lower panel). Both atomic and molecular coherences vanish in the Feshbach insulator (FI) phase.

case), the mean-field energy remains symmetric under the transformation  $\phi_a \rightarrow -\phi_a$ , manifesting the residual  $\mathbb{Z}_2$  symmetry in the choice of the phase of the atomic field. As  $\mu/U$  increases, the metastable BECam minimum is found to jump to the origin  $\phi_a = \phi_m = 0$ , acquiring the nature of a FI (e.g. Fig. 3(c) and (d)), and to become degenerate with the BECam minima for  $\mu/U = -0.23$ . The presence of multiple minima at the transition point is characteristic of a first-order transition.

### FROM FESHBACH INSULATOR TO COLLAPSE FOR BROAD RESONANCES

As mentioned in the main text, increasing the strength  $g$  of the atom-molecule coupling – controlled by the width of the Feshbach resonance – one expects to gradually destabilize the system towards collapse. In particular, a simple scaling argument predicts that the total density increases as  $n \sim (g/U)^2$  when  $g$  increases. In the case of the symmetric atom-molecule mixture ( $t_a = t_m = t$ ,  $U_a = U_m = U_{am} = U$ ) one can conduct a more refined analysis based on an approximate mean-field energy func-

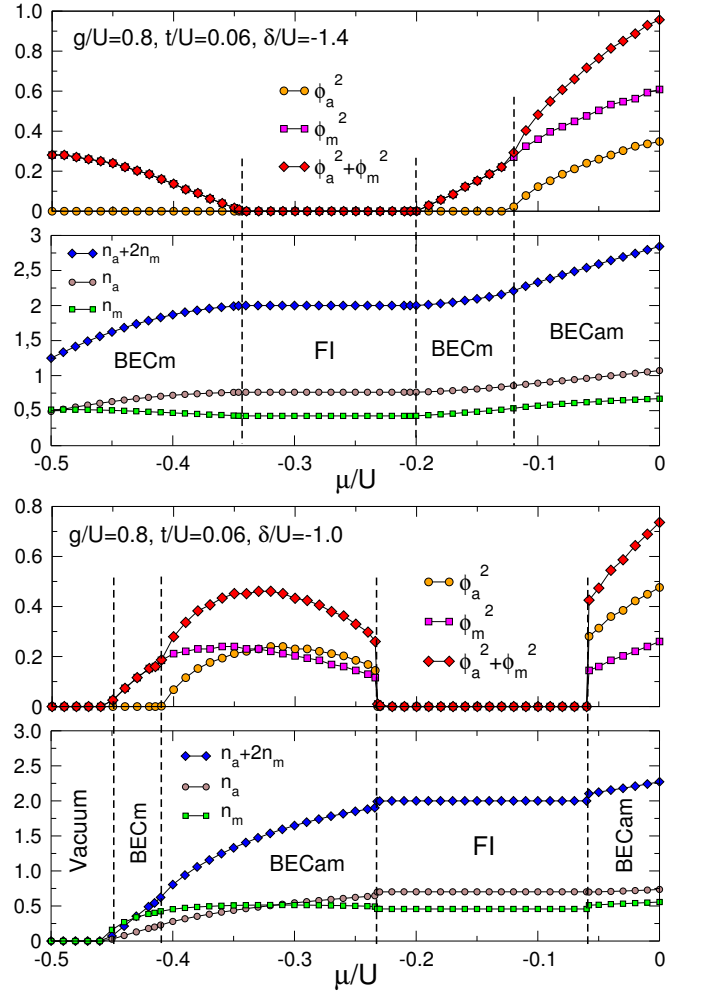


FIG. 2: (Color online) Vertical cuts of the mean field phase diagram (Fig. 2(a) of the main text) for  $\delta/U = -1.4$  (up) and  $\delta/U = -1.0$  (bottom). All the transition are continuous for  $\delta/U = -1.4$ , whereas the atomic-molecular BEC (BECam) to the Feshbach insulator (FI) is first order for  $\delta/U = -1.0$ .

tion, uniquely dependent upon the atomic and molecular densities  $n_a$  and  $n_m$ , and taking the form

$$\mathcal{E}(n_a, n_m) = \frac{U}{2} [n_a(n_a - 1) + n_m(n_m - 1) + 2n_a n_m] - 2gn_a\sqrt{n_m} - \mu(n_a + 2n_m) + (\delta + U)n_m. \quad (2)$$

Here we have neglected the kinetic energy altogether – this is justified in the limit in which  $g$  and  $U$  are the largely dominant energy scales in the system. Moreover, in the conversion term we have assumed a phase difference of  $\pi$  between the atomic and the molecular field, minimizing the conversion energy. In the case  $\mu = 0$ , minimization of the above density function with respect to  $n_a$  and  $n_m$  leads to a rather simple result for the equi-

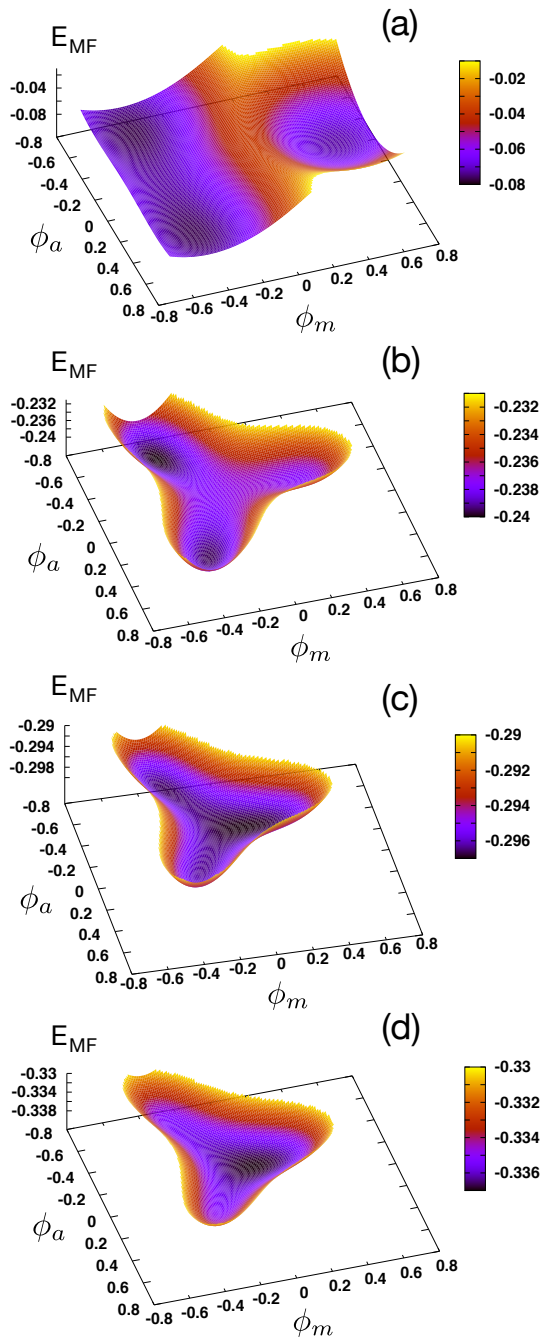


FIG. 3: (Color online) Mean field ground-state energy  $E_{MF}$  with  $g/U = 0.8$ ,  $t/U = 0.06$  and  $\delta/U = -1.0$ . (a)  $\mu/U = -0.35$  (BECam); (b)  $\mu/U = -0.25$  (BECam); (c)  $\mu/U = -0.22$  (FI); (d)  $\mu/U = -0.20$  (FI).

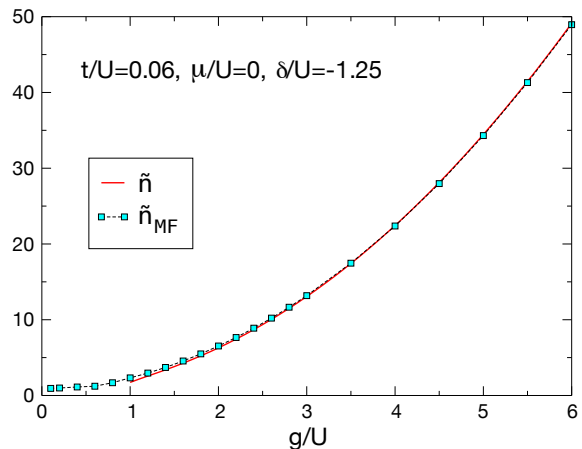


FIG. 4: (Color online) Total number density as a function of  $g/U$  for the 2D atom-molecule symmetric model ( $t_a = t_m = t$ ,  $U_a = U_m = U_{am} = U$ ) with  $t/U = 0.06$ ,  $\delta/U = -1.25$ , and  $\mu = 0$ . The squares indicate the full mean-field solution  $\tilde{n}_{MF}$  (from the minimization of the Hamiltonian Eq. (1)), while the solid line is the prediction from the approximate energy function, Eq. (3).

librium value of the total number density  $\tilde{n} = n_a + n_m$

$$\tilde{n} = \frac{2}{3} \left( \frac{1}{4} + \left( \frac{g}{U} \right)^2 - \frac{\delta}{2U} \right) + \sqrt{\frac{4}{9} \left( \frac{1}{4} + \left( \frac{g}{U} \right)^2 - \frac{\delta}{2U} \right)^2 + \frac{1}{3} \left( 1 + \frac{4\delta}{U} \right)} \quad (3)$$

exhibiting again the anticipated  $(g/U)^2$  scaling. As shown in Fig. 4 the above result reproduces very well the full solution of the self-consistent minimization of the mean-field energy in the case  $t/U = 0.06$  and  $\delta/U = -1.25$ .

Fig. 5 shows the mean-field phase diagram of the symmetric atom-molecule mixture with  $t/U = 0.06$  at fixed  $\delta/U = -1.25$  and variable chemical potential and atom-molecule coupling, reconstructed via the total coherent fraction  $|\phi_a|^2 + |\phi_m|^2$  and the total number density  $\tilde{n} = n_a + n_m$ . The Feshbach insulator for  $n = 2$  is found to persist in the phase diagram only for moderate values of  $g/U$  ( $\sim 1.5$ ), beyond which it leaves space to an atomic-molecular condensate phases with increasing density. Interestingly another incompressible insulating phase is found at (mass) density  $n = 11$  for the particular value of the detuning chosen here - suggesting that in fact a whole family of Feshbach insulators of increasing density might be stabilized in the system - yet a full characterization of the phase diagram upon varying the detuning  $\delta$  goes beyond our current scopes.

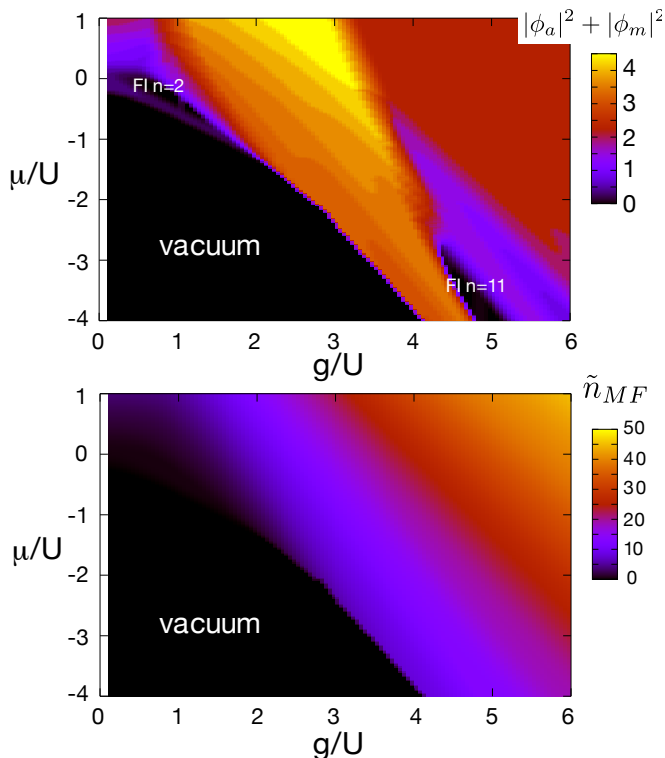


FIG. 5: (Color online) Mean-field phase diagram at  $T = 0$  for the 2D atom-molecule symmetric model ( $t_a = t_m = t$ ,  $U_a = U_m = U_{am} = U$ ) with  $t/U = 0.06$ ,  $\delta/U = -1.25$  upon varying the chemical potential  $\mu$  and the atom-molecule coupling  $g$ . False colours indicate the total coherent fraction (upper panel) and the total mean-field number density (lower panel).

### HAMILTONIAN PARAMETERS FOR A ATOM-MOLECULE RESONANT MIXTURE IN A LATTICE

The Hamiltonian parameters  $t_a, t_m, U_a, U_m, U_{am}$  for  $^{87}\text{Rb}$  atoms and  $^{87}\text{Rb}_2$  Feshbach molecules in a cubic optical lattice, with wavevector  $k$  and depth  $V_0$ , are calculated making use of the numerically calculated band structure and maximally localized Wannier states [1, 2]. The atom and molecule tunnelling matrix element  $t_a$  and  $t_m$  are directly extracted from the width of the lowest energy band. The molecules see an optical lattice of effective depth  $4V_0$ , due to the fact that the dipole matrix element, whose square enters  $V_0$ , takes contribution from both atoms of the molecule. This leads to  $t_a \gg t_m$  (by orders of magnitude), and not to  $t_m = t_a/2$ , as often assumed in the literature.

The on-site atom-atom, molecule-molecule and atom-molecule interactions matrix element, respectively  $U_a$ ,

$U_m$  and  $U_{am}$ , are obtained as

$$U_a = \frac{4\pi\hbar^2 a_{bg}}{m} \int d^3\mathbf{r} |w_a(\mathbf{r})|^4 \quad (4)$$

$$U_m = \frac{16\pi\hbar^2 a_{bg}}{m} \int d^3\mathbf{r} |w_m(\mathbf{r})|^4, \quad (5)$$

$$U_{am} = \frac{8\pi\hbar^2 a_{bg}}{m} \int d^3\mathbf{r} |w_a(\mathbf{r})|^2 |w_m(\mathbf{r})|^2, \quad (6)$$

with  $a_{bg}$  being the background scattering length of the atoms,  $m$  the atomic mass and  $w_{a(m)}(\mathbf{r})$  the atomic (molecular) Wannier function.

The conversion rate between atoms and molecules  $g$  is obtained via the solution of the scattering problem for two atoms in a parabolic potential [3]. Following [4], the parameter  $g$  is given by

$$\frac{g}{U_{a,h}} = \left[ \frac{\sqrt{\pi} m \Delta\mu \Delta B}{\sqrt{2} \hbar^2 k^3 a_{bg}} \left( \left( \frac{V_0}{E_r} \right)^{-\frac{3}{4}} + 0.49 k a_{bg} \left( \frac{V_0}{E_r} \right)^{-\frac{1}{2}} \right) \right]^{\frac{1}{2}} \quad (7)$$

with  $\Delta\mu$  the difference of magnetic moments,  $\Delta B$  the width of the Feshbach resonance,  $V_0$  the lattice depth seen by an atom and  $E_r = \hbar^2 k^2 / 2m$  the atomic recoil energy. Here  $g$  is expressed in units of  $U_{a,h}$ , namely the atom-atom repulsion within the harmonic approximation for the Wannier function,  $U_{a,h} = \sqrt{8/\pi} k a_{bg} (V_0/E_r)^{\frac{3}{4}} E_r$ . For the lattice depth we considered ( $V_0 = 12E_r$ )  $U_{a,h}$  overestimates  $U_a$  by some 20%. Yet this choice of normalization for  $g$  is justified by the fact that  $g$  is also calculated by assuming a single harmonic potential, and hence can be expected to be similarly overestimated with respect to the actual value.

Making contact with the previous section, it is interesting to summarize here our estimates for the value of the  $g/U_{a,h}$  ratio associated with some relevant narrow Feshbach resonances already investigated experimentally [5]. Considering optical lattices of depth  $V_0$  varying between 4 and  $30 E_r$ , we find

1.  $^{87}\text{Rb}$ ,  $B_0 = 414$  G:  $g/U_{a,h} \sim 2 - 1$ ;
2.  $^{23}\text{Na}$ ,  $B_0 = 853$  G:  $g/U_{a,h} \sim 3 - 1$ ;
3.  $^{87}\text{Rb}$ ,  $B_0 = 9$  G:  $g/U_{a,h} \sim 8.5 - 4$ ;
4.  $^6\text{Li}$ ,  $B_0 = 543$  G:  $g/U_{a,h} \sim 7 - 3.5$ .
5.  $^{87}\text{Rb}$ ,  $B_0 = 1007$  G:  $g/U_{a,h} \sim 40 - 20$ ;
6.  $^{23}\text{Na}$ ,  $B_0 = 907$  G:  $g/U_{a,h} \sim 60 - 30$ ;

(Here  $B_0$  indicates the position of the resonance in magnetic field). As already mentioned in the main text, apart from the first two resonances, we cannot find a stable, incompressible Feshbach insulator at density  $n = 2$ . This is consistent with the results of the previous section, which, albeit focusing on an artificially symmetric atom-molecule mixture, were also suggesting that a  $n = 2$  Feshbach insulator is only expected for  $g/U \sim 1$ .

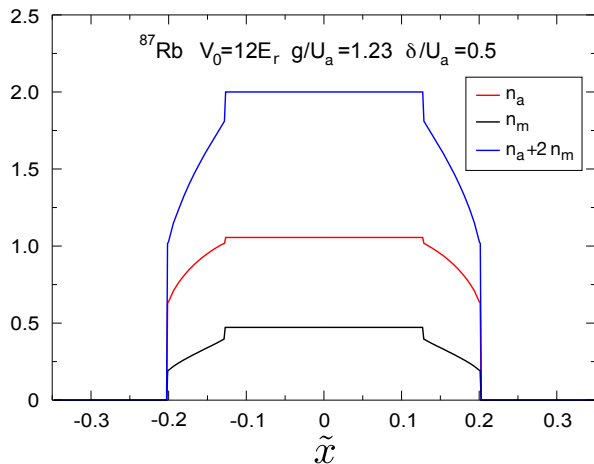


FIG. 6: (Color online) Atomic, molecular and total density profile for  $^{87}\text{Rb}$  in a trap plus cubic optical lattice, with  $\mu/U_a = 0.1$  and  $\delta/U_a = 0.5$ ; other parameters as in Fig. 4(a) of the main text. The abscissa represents the scaled radial variable  $\tilde{x} = V_t/U_a(r/d)^2$ , where  $d$  is the lattice spacing,  $r$  is the radial distance from the trap center, and  $V_t = (1/2)m\omega^2 d^2$  is the trapping potential.

### DENSITY PROFILES FOR NEAR-RESONANT $^{87}\text{RB}$ IN A TRAP

Fig. 6 shows the density profile of  $^{87}\text{Rb}$  in a cubic optical lattice of depth  $V_0/E_r = 12$  plus a harmonic trap, and in a magnetic field close to its 414-G Feshbach resonance. The chemical potential and detuning take values  $\mu/U_a = 0.1$  and  $\delta/U_a = 0.5$ , which sets the trap center into a gapped FI phase with total density  $n = 2$ . The resulting density profile is obtained using standard local-density approximation. Moving towards the trap wings, we observe a density jump in both the atomic and molecular components when the system goes locally from FI to BECam, and a further jump when going from BECam to vacuum. Such jumps are observed as well for square lattices, and they are therefore directly amenable to experimental observation using *e.g.* quantum gas microscopes [6].

### ATOM-MOLECULE COHERENCE FROM MOMENTUM-NOISE CORRELATIONS

The FI is stabilized by atom-molecule conversion, whose characteristic energy dominates all other energy scales in this phase. How to measure atom-molecule conversion energy  $\langle C \rangle = -2g \mathcal{C}$ , where  $\mathcal{C}$  is atom-molecule coherence  $\mathcal{C} = \langle a^2 m^\dagger \rangle$ ?

A possibility is the analysis of the correlations between the noise of atomic and molecular momentum distributions. The momentum distribution of atoms and molecules can be measured simultaneously using Stern-

Gerlach separation during time of flight [7]. This leads us to consider the correlation function

$$G^{(2a,m)}(k, k') = \langle n_a^2(k) n_m(k') \rangle \quad (8)$$

where  $n_a(k)$  and  $n_b(k)$  are the momentum distribution of atoms and molecules respectively.

We assume for simplicity that the state of the system factorises between sites, namely

$$|\Psi\rangle = \bigotimes_{i=1}^N (\cos(\theta/2)|20\rangle + \sin(\theta/2)|01\rangle) \quad (9)$$

where the state is expressed in the  $|n_a n_m\rangle$  basis.

Then we readily obtain that

$$G^{(2a,m)}(k, k') = 2\langle n_a^2 \rangle \langle n_m \rangle + \frac{n_m n_a}{N} + \frac{|\mathcal{C}|^2}{N} \delta_{2k-k', K} + \mathcal{O}\left(\frac{1}{N^2}\right) \quad (10)$$

where  $n_a, n_m$  are the average atomic and molecular densities,  $K$  is a reciprocal lattice vector, and  $\mathcal{C} = (\sin \theta)/2$ .

Introducing then the function

$$g_{2a,m}^{(2)}(q) = \frac{\sum_k G^{(2a,m)}(k, 2k+q)}{\sum_k \langle n_a^2(k) \rangle \langle n_m(2k+q) \rangle} \quad (11)$$

we find that, for the factorized state of Eq. (9)

$$g_{2a,m}^{(2)}(q) = 1 + \frac{|\mathcal{C}|^2}{2n_a^2 n_m} \frac{1}{N} \delta_{q,K} + \mathcal{O}\left(\frac{1}{N^2}\right) \quad (12)$$

namely this function exhibits a series of *bunching peaks* describing the reciprocal lattice, and whose height is proportional to the square of the atom-molecule coherence. Hence the noise correlations in the fluctuations of the atomic and molecular momentum distributions reveal the presence of atom-molecule coherence. Yet an important limitation of this approach is that the bunching peaks are suppressed like  $1/N$ . This means that the bunching signal can only be seen on relatively *small samples* – as it is a factor of  $N$  weaker than the typical bunching signal of a Mott insulator in a very deep optical lattice, as detected *e.g.* in [8].

### FURTHER INFORMATION

1. The restriction to a single band is justified as long as the atom-molecule conversion term  $g$  is significantly smaller than the band gap. This is verified in all our calculations;
2. The FI phase exists in  $D = 1$  as well, but it has not been discussed in the previous literature;
3. Obviously the BECam phase is characterised by condensation of atom *pairs*, whose phase is fixed by the molecular field;

4. In Fig. 2(a) of the main text, the FI appears for  $\delta/U \lesssim -1$ , namely on the molecular side of the (on-site) resonance. This is easily understood by looking at the case  $g = 0$ : in the system at hand the relevant states coupled by the  $g$  terms are a BECa and a BECm, whose degeneracy is not reached for  $\delta = 0$  but for  $\delta < 0$  ( $\delta = 0$  would be the resonance condition between atomic and molecular MI). The shift of the resonance to negative  $\delta$  stems from the mismatch in kinetic energy between atoms and molecules (in the case at hand, even if  $t_a = t_m$  the molecules are - at most - half the number the atoms); to stabilize a molecular state, the increase in kinetic energy has then to be compensated by a negative detuning;
5. Indeed, let us consider a particle-hole excitation from a two-site state  $[(|20\rangle + |01\rangle)/\sqrt{2}]^{\otimes 2}$  to a state  $[(|30\rangle + |11\rangle)/\sqrt{2} \otimes |10\rangle$  (where the states are expressed in the  $|n_a n_m\rangle$  basis). The conversion energy goes from  $-2\sqrt{2} g$  to  $-\sqrt{6} g$ , whence the particle-hole gap;
6. In this case, the composite  $U(1) \times Z_2$  symmetry is coming from the molecular phase and the atomic phase, respectively. Interestingly, first-order transitions are generically found in  $D + 1 = 3$  dimensions when the breaking of a  $U(1) \times Z_2$  symmetry is involved [9, 10];
7. We have considered several other narrow Feshbach resonances for various atomic species, namely:  $^{87}\text{Rb}$  (resonances at 9 G, and 1007 G),  $^{23}\text{Na}$  (907 G),  $^6\text{Li}$  (543 G) [5]. Yet only the above cited ones turn out to be sufficiently narrow for the appearance of a stable FI phase with  $n = 2$ ;
8. Here  $E_r = h^2/2m\lambda^2$  is the recoil energy for particles of mass  $m$  in a laser wave of wavelength  $\lambda$ ; we chose  $\lambda = 830$  nm;
9. A similar behavior is also observed in the mean-field phase diagram of  $^{23}\text{Na}$  around its 853 G resonance;
10. The normalization of the momentum distribution is such that  $n(k)d^D k$  gives the number of particles in the infinitesimal volume  $d^D k$  of momentum space;
11. It is interesting to observe the non-monotonic behavior of the atomic coherence as  $\delta$  is reduced towards the resonance: the coherence peak is enhanced first – as expected from the reduction of the effective scattering length – but then it is suppressed, owing to the localizing effect of the resonant atom-molecule conversion term; In a real experiment, an adiabatic sweep in  $\delta$  should lead to hysteresis, namely to a history-dependent form of the momentum distribution depending on whether the detuning is swept across the transition coming from the molecular or the atomic side.

---

[1] U. Bissbort, Dissertation, urn:nbn:de:hebis:30:3-285913 (2012).

[2] M. Greiner, Dissertation, urn:nbn:de:bvb:19-9683 (2003).

[3] Th. Busch, B.-G. Englert, K. Rzazewski, and M. Wilkens, *Found. Phys.* **28**, 549 (1998).

[4] N. Syassen, D. M. Bauer, M. Lettner, D. Dietze, T. Volz, S. Dürr, and G. Rempe, *Phys. Rev. Lett.* **99**, 033201 (2007).

[5] C. Chin, R. Grimm, P. Julienne, and E. Tiesinga, *Rev. Mod. Phys.* **82**, 1225 (2010).

[6] W. S. Bakr, J. I. Gillen, A. Peng, S. Foelling, and M. Greiner, *Nature* **462**, 74 (2009).

[7] J. Herbig, T. Kraemer, M. Mark, T. Weber, C. Chin, H.-C. Nägerl, and R. Grimm, *Science* **301**, 1510 (2003).

[8] S. Fölling, F. Gerbier, A. Widera, O. Mandel, T. Gericke and I. Bloch, *Nature* **434**, 491 (2005).

[9] V. Thanh Ngo and H. T. Diep, *J. Appl. Phys.* **103**, 07C712 (2008).

[10] A. O. Sorokin, *JETP* **118**, 417 (2014).